



HAL
open science

Hydroconversion of Octylcyclohexane over a Bifunctional Pt/USY Zeolite Catalyst

Larissa Brito, Gerhard D. Pirngruber, Emmanuelle Guillon, Florian Albrieux,
Johan A. Martens

► **To cite this version:**

Larissa Brito, Gerhard D. Pirngruber, Emmanuelle Guillon, Florian Albrieux, Johan A. Martens. Hydroconversion of Octylcyclohexane over a Bifunctional Pt/USY Zeolite Catalyst. *Energy & Fuels*, 2021, 35 (17), pp.13955-13966. 10.1002/cctc.201902372 . hal-03356051

HAL Id: hal-03356051

<https://ifp.hal.science/hal-03356051>

Submitted on 27 Sep 2021

HAL is a multi-disciplinary open access archive for the deposit and dissemination of scientific research documents, whether they are published or not. The documents may come from teaching and research institutions in France or abroad, or from public or private research centers.

L'archive ouverte pluridisciplinaire **HAL**, est destinée au dépôt et à la diffusion de documents scientifiques de niveau recherche, publiés ou non, émanant des établissements d'enseignement et de recherche français ou étrangers, des laboratoires publics ou privés.

Hydroconversion of octylcyclohexane over a bifunctional Pt/USY zeolite catalyst

Larissa Brito¹, Gerhard D. Pirngruber*¹, Emmanuelle Guillon¹, Florian Albrieux¹, Johan A.
Martens²

¹ IFP Energies nouvelles, Rond Point de l'échangeur de Solaize, 69360 Solaize, France

² KU Leuven, Center for Surface Chemistry and Catalysis, Celestijnenlaan 200F, 3001
Leuven, Belgium

Corresponding author: Gerhard Pirngruber, IFP Energies nouvelles, Rond Point de
l'échangeur de Solaize, BP-3, 69360 Solaize, France. Email : gerhard.pirngruber@ifpen.fr

Keywords: USY, bifunctional catalysis, hydroisomerization, hydrocracking, naphthene,
Paring reaction

ABSTRACT

Hydroisomerization and hydrocracking of octylcyclohexane (C₁₄H₂₈), obtained after *in situ* hydrogenation of the parent aromatic compound, phenyloctane (C₁₄H₂₂), on a Pt/Al₂O₃ pre-catalyst, were performed over a bifunctional Pt/USY zeolite catalyst, at 573 K, 6 MPa and a molar ratio H₂/HC of 7 mol/mol. About 200 reaction products were identified and quantified with GCxGC-FID/MS and then lumped into families according to carbon number and chemical similarity. Insight in reaction pathways was gained from the evolution of the composition of the isomers and cracked products with conversion. The results illustrate a kinetic competition between isomerization steps, which increase the number of branchings on the ring by shifting carbon atoms from the long alkyl chain to the ring, with exo-cyclic cracking of the long alkyl chain. Favorable cracking distributions are reached as soon as the molecule is tri-branched, which leads to a peak at C7 in the product distribution.

27 1 Introduction

28 Hydrocracking is a versatile process serving the conversion of heavy oil fractions, mainly
29 Vacuum gas oil (VGO), to desired products, such as diesel and jet fuel¹⁻⁶. VGO cuts are rich
30 in cyclic molecules, i.e. aromatics and naphthenes, in addition to aliphatic hydrocarbons^{7,8}.
31 Hydroconversion mechanisms of alkanes have been exhaustively reported in literature⁹⁻¹³ and
32 follow a bifunctional reaction pathway^{14,15} over metal supported zeolite or amorphous oxide
33 based catalysts. The reaction steps comprise dehydrogenation of the feed over metal sites of the
34 bifunctional catalyst, diffusion of the generated olefin towards acidic sites, protonation and
35 rearrangement and cracking of the reaction intermediates on the acidic sites, and desorption and
36 diffusion of the isomerized or cracked olefins towards the metal sites of the catalyst, where they
37 undergo hydrogenation. In the absence of shape-selectivity effects, i.e. for large pore zeolite
38 catalysts, the rates of isomerization and cracking steps of alkanes depend on the stability of the
39 alkylcarbenium ions involved. The product distribution can be fairly well rationalized and
40 predicted based on carbocation chemistry. This also holds true for long-chain alkanes, which
41 are within or close to the VGO boiling range^{10,11,16,17}.

42 The hydrocracking chemistry of heavy naphthenes has been much less studied than that of long-
43 chain alkanes. Several practical limitations restrict the size and type of naphthenic molecules
44 that can be employed as model compound for kinetic studies. Many recent studies focused on
45 the hydroconversion of decalin in the context of selective ring opening, i.e. with bifunctional
46 catalyst with very high metal loadings, having a high hydrogenolysis activity. Under such
47 conditions the metal assumes a cracking function that is beneficial for the purpose of selective
48 ring opening of compounds like decaline¹⁸⁻³¹. Here, we only consider bifunctional catalysts
49 where the metal function only serves hydrogenation-dehydrogenation to feed the acid sites with
50 olefins. Hydrocracking studies of this kind have been dealing with naphthenes presenting three
51 cycles³²⁻³⁵, two cycles³⁶⁻⁴⁰ or one cycle⁴¹⁻⁴³. It has been shown that the hydroisomerization

52 and hydrocracking mechanisms of cyclic molecules follow similar principals as for the
53 hydroconversion of alkanes with respect to relative stabilities of involved alkylcarbenium ions,
54 but the presence of rings leads to distinctly different product distributions ⁴⁴. Rearrangements
55 of the naphthenic cycle comprise alkyl-shifts, ring-contraction and expansion, which may
56 change the degree of branching of the molecule. Naphthenes may contract or expand their cycle
57 through Protonated Cyclo Propane (PCP) intermediates ⁵. This PCP-type transition state is also
58 involved in positional alkyl-shifts that take place around the cycle (endocyclic alkyl-shifts) and
59 that move carbons towards the substituent alkyl-chain (exocyclic alkyl-shifts). Finally, there is
60 also a possibility of creating a branching in an alkyl-chain substituent of the ring through a PCP
61 intermediate. Activation energies of all these skeletal rearrangements have been reported in
62 literature ⁴⁵.

63 Monocyclic naphthenes undergo isomerization of the cycle, i.e. ring-contraction or expansion,
64 without opening it. The opening of the unique ring of a monocyclic naphthene is considered to
65 be a difficult reaction step, due to orbital hindrance ⁴⁶. The main consequence of this strained
66 reaction is that the alkylcarbenium ion of a substituted monocyclic naphthene undergoes
67 skeletal branching of its ring and of its alkyl chains until a favorable configuration of branchings
68 and the positively charged C-atom is achieved to enable fast beta-scission. This catalytic
69 chemistry has been observed for naphthenes containing 9 to 12 carbon atoms and it is called
70 “paring” reaction ⁴². Egan *et al.* observed that a substituted C₁₀ naphthene would crack
71 selectively to cyclic C₆ (cyclohexane or methylcyclopentane) and isobutane, irrespective of the
72 starting naphthene isomer. C₁₁ and C₁₂ naphthenes (pentamethyl- and hexamethylcyclohexane)
73 also mainly cracked into isobutane and a corresponding substituted naphthene with 7 or 8
74 carbon atoms, respectively ⁴². The formation of isobutane can be rationalized by a series of
75 alkyl shifts on the ring and ring contractions (both of which are very fast reactions), leading to
76 the formation of a tert-butyl side chain, which can then very easily undergo beta-scission.

77 Souverijns *et al.* studied the hydroisomerization of a C₁₄ naphthene with a long alkyl side chain,
78 viz. octylcyclohexane, over a Pt/USY bifunctional catalyst⁴⁷. The catalyst quickly generated a
79 distribution of naphthene isomers with mainly di- and mono-substituted rings. The distribution
80 of isomers indicated that methyl branching of the alkyl chain was kinetically favored at carbon
81 positions close to the ring. Methyl groups on the ring were formed through ring-contraction,
82 and shifted to the long alkyl side chain, where after the ring expanded again by incorporation a
83 C atom of the long alkyl chain. In other words, branchings were generated on the ring and
84 propagated towards the long alkyl-substituent. This reaction pathway was faster than direct
85 methyl branching of the long alkyl chain.

86 The reaction conditions in the paper by Souverijns *et al.*⁴⁷ were very mild, so the feed
87 molecules were only isomerized, but not cracked. Hence, there is no documented study on the
88 hydrocracking behavior of naphthenes with long alkyl-chain substituent. Such information is
89 clearly needed to understand better the hydrocracking behavior of real feeds like VGO, since
90 the analyses of VGO suggests that the naphthenes in this feed are heavily alkyl substituted and
91 must, statistically, contain quite long alkyl chains in view of their molecular mass^{48,49}.

92 Therefore, after having studied in previous work the reaction pathway of the tricyclic molecule
93 perhydrophenanthrene⁴⁹, we address here the bifunctional catalytic conversion of
94 octylcyclohexane (C₁₄H₂₈) as a long-chain substituted monocyclic naphthene. In order to
95 provide mechanistic insights in its isomerization and hydrocracking reaction pathways on a
96 bifunctional Pt/USY zeolite catalyst, we identified in great detail the distribution of
97 isomerization products by the use of GCxGC-MS analysis, and related them to the resulting
98 cracking products, so as to elucidate the reaction network.

99

100 2 **Materials and methods**

101 2.1 Preparation and characterization of catalysts

102 Commercial ultrastable Y zeolite (CBV720) with bulk Si/Al ratio of 17.7 and a Brønsted acid
103 site concentration of 202 $\mu\text{mol/g}$ according to pyridine adsorption and quantification with FTIR
104 was supplied in powder form by Zeolyst. The zeolite was shaped into extrudates with alumina
105 binder (Pural SB3) provided by Sasol, according to procedures described elsewhere⁵⁰. The
106 shaped catalyst contained 1 wt.% of USY zeolite. Pure alumina extrudate without zeolite was
107 also prepared. In both cases, the length range of the cylindrical extrudates was 3-6 mm, and the
108 diameter 1.6 mm. Calcination was performed at 793 K during 2 h according to the protocol
109 used previously⁵⁰. The main motivation for using extrudates was (i) to obtain a well-defined
110 packing of the catalyst bed and, thus, a well-defined hydrodynamics and (ii) to dilute the zeolite
111 in catalyst bed in a homogeneous way. A strong dilution was necessary in order to be able to
112 reach reasonably low conversion values with the very active USY catalyst.

113 Impregnation of the extrudates with platinum was carried out using chloroplatinic acid
114 (H_2PtCl_6 , Sigma-Aldrich). The PtCl_6^{2-} complex exhibits a strong ionic interaction with the
115 alumina support and should be preferentially adsorbed on the latter (and not in the USY
116 crystals)⁵¹. We are aware the impact on Pt location on activity and selectivity in bifunctional
117 hydrocracking reactions is still subject to debate, but it is beyond the scope of the present article
118 to fully address this issue⁵²⁻⁵⁵. A complete procedure of the impregnation process, as well as
119 thermal treatments applied on the final catalysts, may be found in previous work⁵⁰.

120 The Pt content of the final catalysts was determined using X-ray fluorescence. The Pt dispersion
121 and size of Pt particles, considering a spherical shape were determined using hydrogen-oxygen
122 titration. The Pt content was 0.65 wt.-%, and the Pt dispersion 45% leading to a concentration
123 of accessible Pt atoms of ca. 9 $\mu\text{mol/g}$ and the average Pt particle size 2.5 nm. The content of

124 Brønsted acid sites assuming that the native USY zeolite was not affected by the shaping
125 procedure^{13,56} was ca. 2 $\mu\text{mol/g}$.

126 2.2 Catalytic experiments

127 Hydroconversion of octylcyclohexane was performed in a fixed-bed down flow reactor with
128 internal diameter of 19 mm, at a total pressure of 6 MPa. Phenyloctane ($\text{C}_{14}\text{H}_{22}$, Alfa Aesar)
129 was diluted into n-heptane (AnalaR Normapur) in a proportion of 5/95 wt.-%. The parent
130 aromatic was used because of the difficulty of obtaining its corresponding naphthene
131 commercially. It was hydrogenated in situ to octylcyclohexane ($\text{C}_{14}\text{H}_{28}$) by a hydrogenation
132 catalyst, which was placed on top of the catalytic bed. A high molar ratio of hydrogen to total
133 hydrocarbons (reactant + solvent) of 7 mol/mol was used to prevent coke formation, and
134 guarantee the full conversion of phenyloctane to octylcyclohexane on the hydrogenation pre-
135 catalyst. Two catalysts were, thus, loaded into the reactor in layers, viz., 2 g of Pt/Alumina pre-
136 catalyst extrudates upstream of 2 g of extrudates of bifunctional Pt/USY zeolite catalyst. Both
137 catalyst beds underwent *in situ* activation by reduction with hydrogen gas, as described in our
138 previous work⁵⁰. The conversion was varied by changing the WHSV, expressed as mass flow
139 of liquid divided by the mass of Pt/USY extrudates. The majority of the catalytic tests were
140 carried out at 573 K. We note that the suitable temperature window for the experiments was
141 constrained by experimental limitations (problems of operability at lower temperatures),
142 thermodynamic limitations (full hydrogenation of aromatics) and also our ambition to keep the
143 conditions close to our previous work on perhydrophenanthrene⁵⁰.

144 Finally, we comment on the choice of the solvent. Ideally, the solvent should be inert under the
145 reaction conditions. That is why we opted for a relatively short n-paraffin, which does not
146 readily, crack, i.e. n-heptane. However, as will be discussed later, we cannot exclude that some
147 isomerization of n-heptane took place in parallel to the hydroconversion of octylcyclohexane,
148 which led to some complications in the product distributions.

149 Deactivation of the catalyst was not observed in the range of operating conditions tested. The
150 absence of external diffusion limitations in the reactor had been verified by comparing results
151 obtained at the same space velocity, but different flow rates. Strong activity differences to other
152 catalysts (factor 0.5 in activity vs. zeolite Beta, factor 3 vs. silica-alumina⁵⁷) further confirmed
153 that we were probing catalytic effects, with little or no impact of mass transfer towards the
154 zeolite particles.

155 2.3 Analysis of reaction products

156 Liquid effluents were condensed and separated from the gaseous reaction products. The gas
157 phase was analyzed online by GC. The liquid reaction products were withdrawn from the
158 separator in regular intervals and analyzed by two-dimensional gas chromatography, with an
159 apolar column (HP PONA) for the first dimension and a polar column (BPX50) for the second
160 dimension. The gas chromatograph was coupled either to a time of flight mass spectrometer
161 (TOF/MS provided by LECO) or to a flame ionization detector (FID). Detailed procedure
162 regarding this setup is available in our previous publication⁵⁰.

163 Both GC columns were operated using the same temperature program, starting from 313 K,
164 with a holding time of 5 minutes, heating to 393 K at 1.5K/min, subsequently to 408 K at
165 0.75K/min, holding 10 min at this temperature; next to 433 K at 0.75K/min, holding 5 min at
166 this temperature; and finally to 503K, at 5K/min, holding 5 min at the final temperature. 1 μ L
167 of the reaction effluent was injected with a split ratio of 1:100. High-purity helium was used as
168 carrier gas at a constant rate of 10 mL/min. By combining the gas and liquid phase analyses,
169 mass balances between 95 and 97 % were achieved.

170 For presenting the results, i.e. for calculating conversion and selectivities, material balances
171 were expressed on a carbon mole basis (which is very close to a weight basis, but provides more
172 insights). For expressing product distributions within a given family, however, it was more

173 convenient to use molar ratios instead of moles of carbon. The error margin of the reported
174 conversions is about +/- 5%.

175 3 **Results**

176 3.1 Hydrogenation of phenyloctane to octylcyclohexane

177 The parent aromatic compound, phenyloctane, was hydrogenated *in situ* over the Pt/Al₂O₃ pre-
178 catalyst. GC analysis confirmed that at a reaction temperature of 573 K its hydrogenation to
179 naphthene was complete. Next to hydrogenation, the pre-catalyst performed some ring
180 contraction and side chain elongation, i.e. it converted part of the octylcyclohexane to
181 nonylcyclopentane. The chromatographic peaks of these two compounds strongly overlapped.
182 Therefore, the conversion of octylcyclohexane to nonylcyclopentane on the pre-catalyst could
183 not be precisely evaluated, but was estimated to be less than 5%. This mixture constituted the
184 reactant undergoing hydroisomerization and hydrocracking over the bifunctional Pt/USY
185 zeolite catalyst mounted downstream in the reactor. For convenience, hereafter the reactant will
186 be referred to as octylcyclohexane (OCC6), knowing there is some nonylcyclopentane present
187 as well.

188 3.2 Identification and quantification of reaction products with GCxGC – FID/MS

189 GCxGC-FID analysis of reaction products obtained over the Pt/USY catalyst is illustrated in
190 Figure 1. The reaction products obtained at 71% octylcyclohexane conversion comprised over
191 200 individually identified compounds. Naphthenes with two and more alkyl substituents have
192 many positional isomers, and may have different diastereomers. The analytical technique did
193 not provide information on positional isomers and diastereomers. In this discussion of
194 bifunctional catalysis the molecules are presented by the nature of the alkyl substituents without
195 specifying the positions on the naphthene ring.

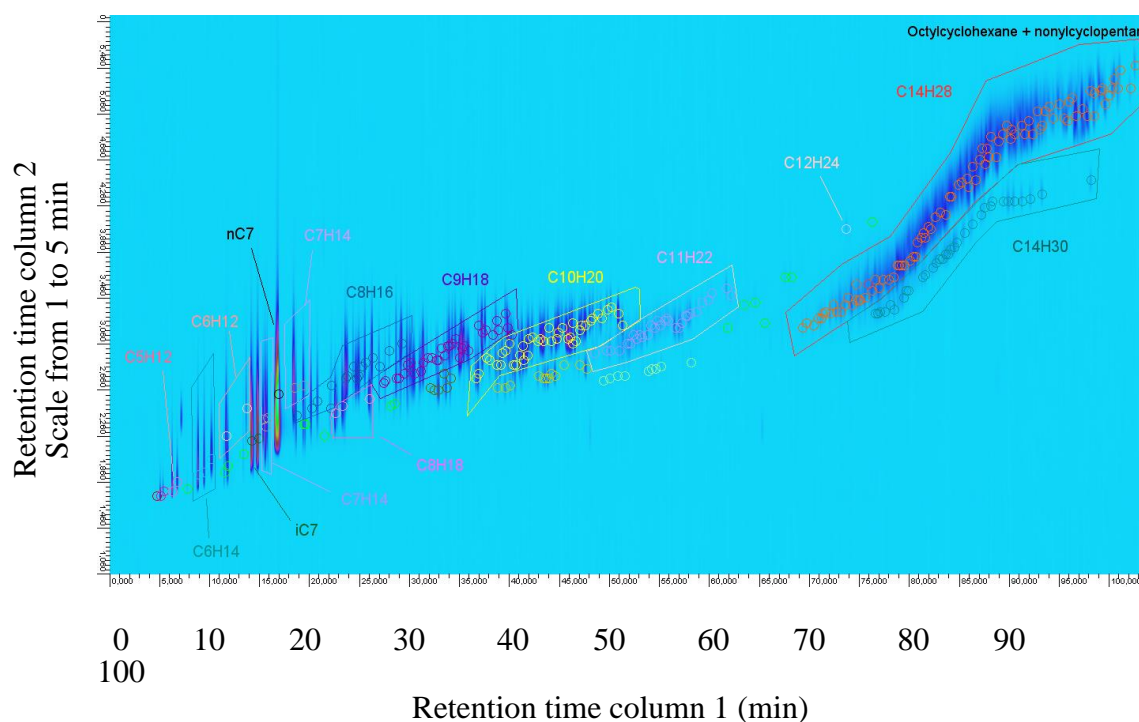


Figure 1. GCxGC-FID analysis of reaction products at 71% conversion of octylcyclohexane over Pt/USY zeolite catalyst.

196 Reaction products were lumped into different groups according to their carbon number and
 197 chemical structure (Figure 2). Isomers of octylcyclohexane ($C_{14}H_{28}$) were divided into
 198 substituted cyclohexanes and cyclopentanes, respectively. Among the $C_{14}H_{28}$ isomers, some
 199 molecules had a high number of branchings. For convenience, a tertiary carbon is considered
 200 to represent one branching, and a quaternary carbon atom two branchings. The most branched
 201 isomer shown in Figure 2 has 6 branchings.

202 Ring-opening products ($C_{14}H_{30}$), i.e., alkanes containing 14 carbon atoms, were detected only
 203 in small amounts and were mono or dimethyl-branched. The opening of a naphthenic cycle is
 204 known to be a difficult reaction⁴⁶. Reaction products containing less than 14 carbon atoms were
 205 assigned as cracking products and divided into naphthenes, n- and iso-alkanes.

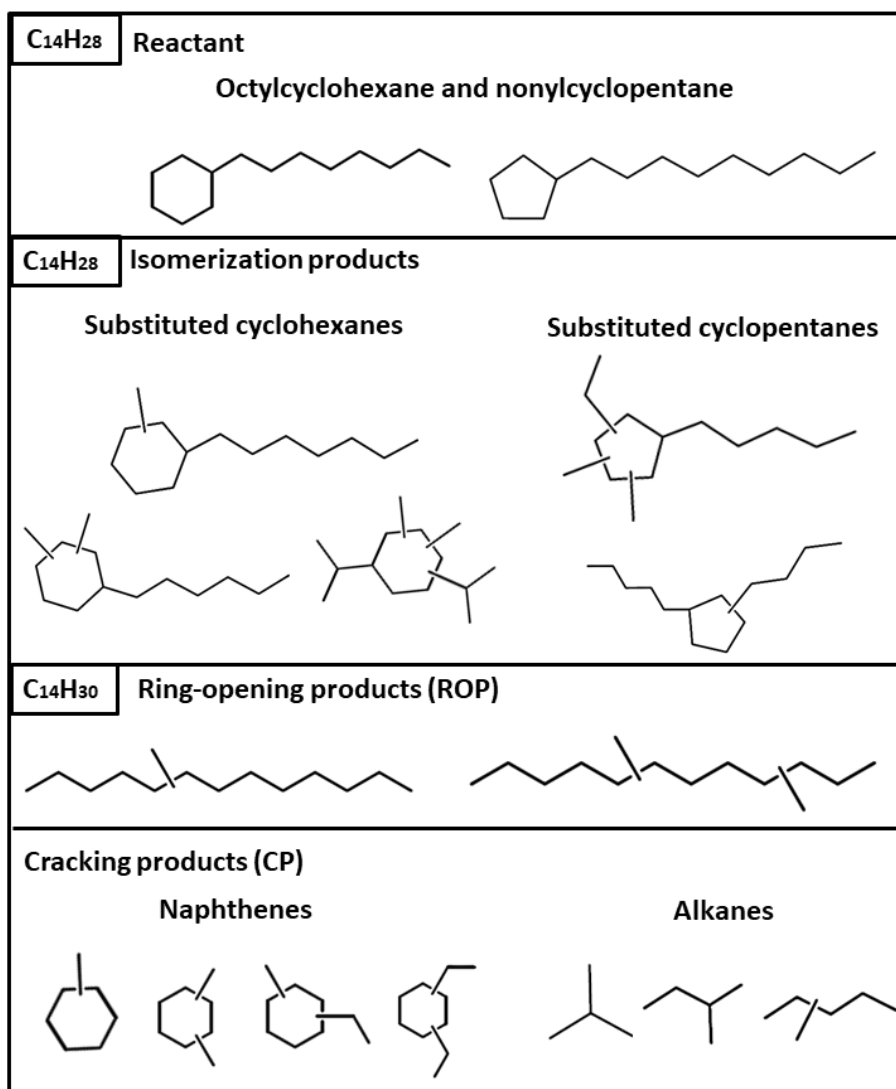


Figure 2. Molecule families and typical examples of molecules in the reaction products of hydroconversion of octylcyclohexane over Pt/USY zeolite catalyst.

206 Since the n-heptane solvent is much lighter than our reactant, we expect it to have a very low
 207 reactivity compared to octylcyclohexane. However, a comparative test with methyl-
 208 cyclohexane as solvent showed that some iso-heptane originated from isomerization of the
 209 solvent when n-heptane was used. Instead of trying to subtract the contribution of the solvent,
 210 which would have been an exceedingly difficult task, we decided to ignore iso-heptanes as
 211 reaction products. Hydrocracking of n-heptane to smaller alkanes did not happen to a significant
 212 extent, since it should produce large amount of propane and, as we will show later, only very
 213 little propane was detected among the products (and its amount did not depend on the solvent).

214 3.3 Hydroconversion of octylcyclohexane

215 Variation of the conversion of octylcyclohexane in a range from ca. 48% to 86% was obtained

216 by changing the contact time at a reaction temperature of 573 K (Figure 3).

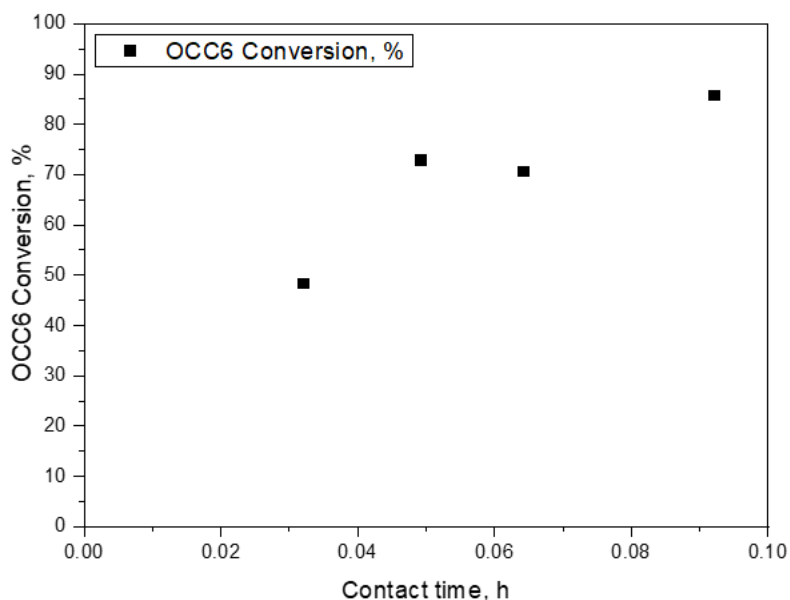


Figure 3. Evolution of octylcyclohexane conversion at 573 K with contact time, expressed as 1/WHSV.

217 The selectivity to isomerization, ring-opening and cracking is given in Figure 4. The curves

218 suggest that isomerization reactions are primary, while cracking reactions are secondary, as

219 expected in bifunctional catalysis^{44,58}. The primary nature of the isomerization products is

220 confirmed by low conversion data obtained with less active catalysts⁵⁷. Selectivity to ring-

221 opening products accounted for less than 1% at all conversion degrees. Opening of a naphthene

222 cycle is known to be a difficult reaction.

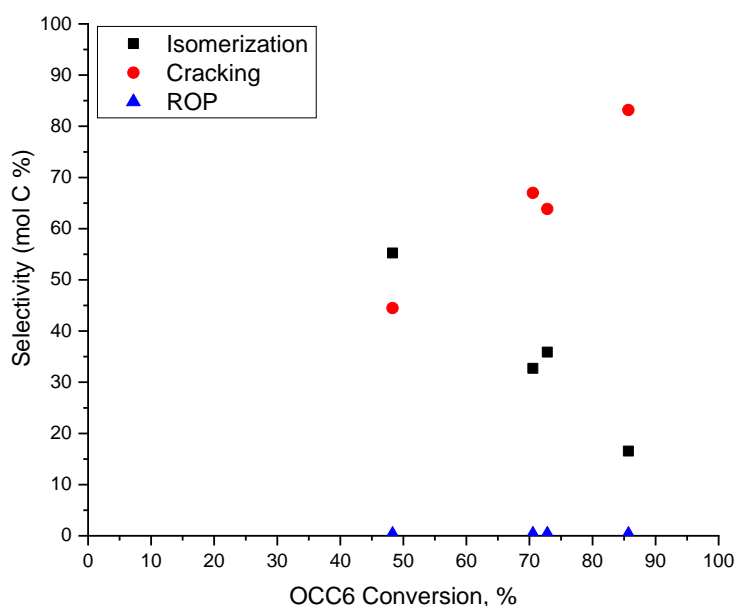


Figure 4. Selectivity to isomers, ring-opening products (ROP) and cracked products as a function of octylcyclohexane conversion.

223 The distribution of $C_{14}H_{28}$ isomers as a function of octylcyclohexane conversion over Pt/H-
 224 USY zeolite catalyst is shown in **Figure 5**. Several compounds presenting different degrees of
 225 branching were identified. The isomers with the longest alkyl side chains were **I2** (di-
 226 substituted), **I8** (minority product, which can arise from ring-contraction of **I2**) and **I7** (tri-
 227 substituted). **I4** (di-substituted) and **I6** (tetra-substituted) were ring contraction isomers with C_5
 228 side chains. The other isomers, which could be identified (**I1**, **I3** and **I5**) were highly substituted
 229 and had only short (sometimes branched) alkyl side chains. **I2** was the most abundant isomer,
 230 in line with the findings of ref. ⁴⁷. Its concentration decreased with conversion, indicating that
 231 it was the primary isomerization product which was then probably converted to other isomers.
 232 The unknown fraction accounted for 20 % of the distribution in average. In contrast to the
 233 results of Souverijns et al. ⁴⁷, we did not identify any mono-substituted naphthenes with
 234 branched side chains. In that study, the degree of conversion of octylcyclohexane was kept
 235 limited to investigate the primary products. Here, at conversions of 48% and higher, the isomers

236 are the result of many consecutive skeletal rearrangements. It is remarkable that the branching
 237 degree of the isomers can be very high. For instance, compound **I3** has six tertiary C-atoms,
 238 accounting for six branchings. In the conversion of long alkanes, the skeletal isomerization
 239 leads to the introduction of three branching at the maximum, because at that stage the molecule
 240 becomes very sensitive to cracking.

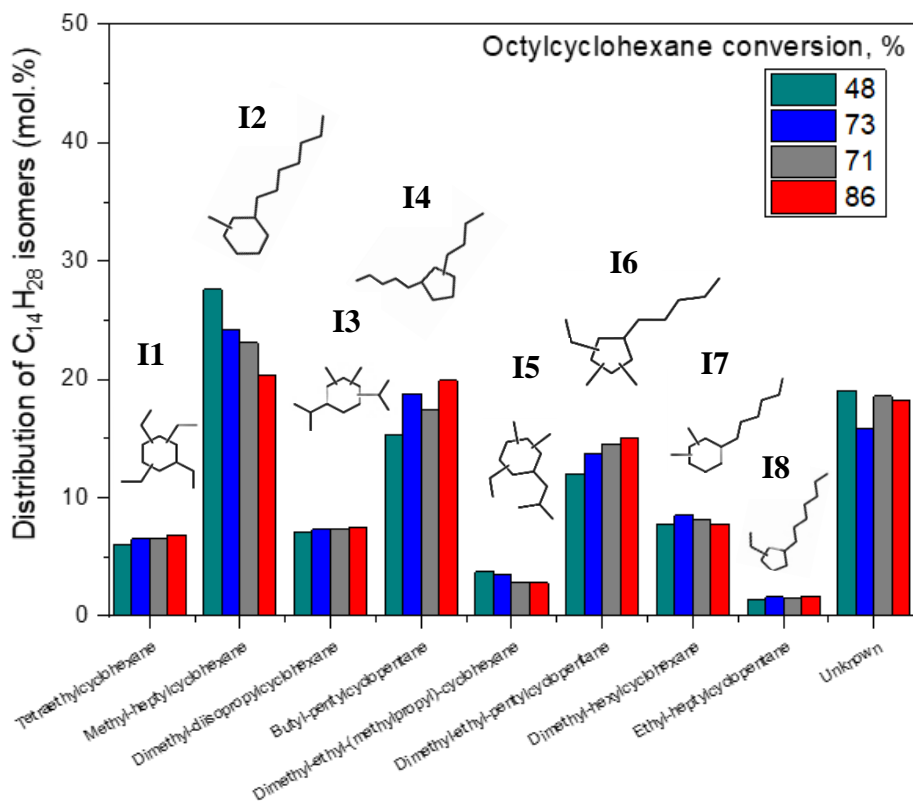


Figure 5. Distribution of octylcyclohexane isomers at different conversion levels.

241 The molar yield of cracked products, grouped according to carbon number, per 100 mol of
 242 cracked feed molecules is presented in Figure 6. Cracked products covered mainly a range of
 243 carbon numbers from 4 to 10, with smaller amounts of C₃ and C₁₁ and trace formation of C₁,
 244 C₂ and C₁₂. The distributions showed a pronounced maximum at C₇ compounds,
 245 notwithstanding the fact that the C₇ formation was underestimated, since only cyclic molecules
 246 could be accounted for (iso-C₇ alkanes were not counted since they might stem from the n-
 247 heptane solvent). About equal molar amounts of C₄, C₅, C₆, C₈, C₉ and C₁₀ were formed by

248 hydrocracking at the four investigated conversion levels. Methane and ethane formation is
249 ascribed to hydrogenolysis^{26,59}.

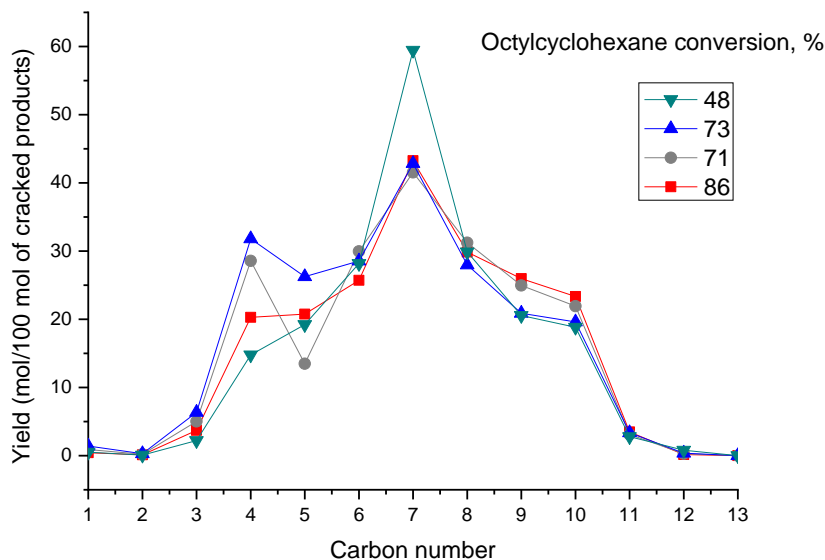


Figure 6. Moles of cracked products per 100 mol of cracked octylcyclohexane at different levels of octylcyclohexane conversion. The sum of molar yields of cracked products per 100 mol OCC6 cracked (Total Yc) is indicated.

250 Cracked products comprised naphthenes, isoalkanes and n-alkanes. Their distribution given in
251 Figure 7 did not change much with conversion. In absence of ring opening, the cracked products
252 are expected to contain an equimolar mixture of naphthenes and alkanes. In the distribution of
253 Figure 7, naphthenes represent more than 50 mol-% of the cracked products. This is a result of
254 the problem with the analysis of the C₇ fraction, and the fact that C₇ isoalkanes were not counted
255 as reaction products because they could not be distinguished from the solvent and its branched
256 impurities.

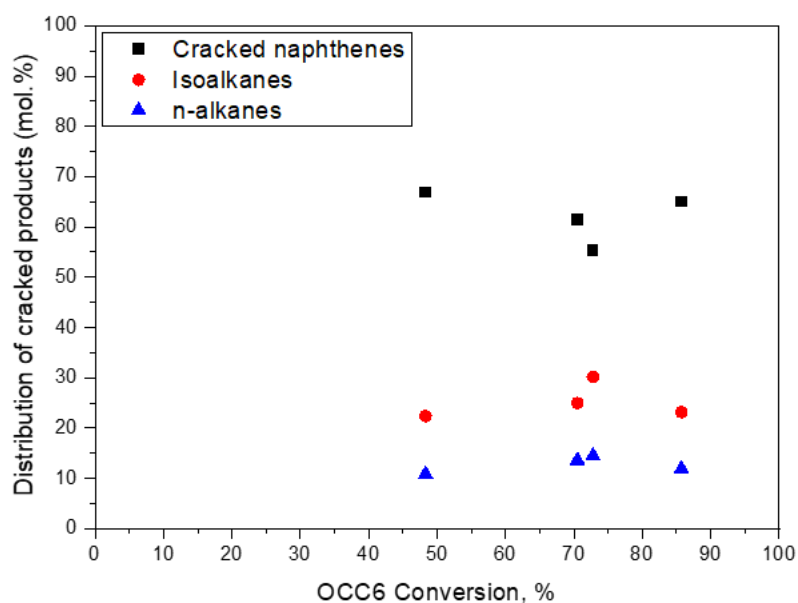


Figure 7. Distribution of cracked products as a function of octylcyclohexane conversion.

257

258 The molar distribution of naphthene cracked products is shown in Figure 8. C₇ naphthenes were
 259 the major products. Their percentage slightly decreased with conversion. C₈, C₉ and C₁₀ cyclic
 260 molecules were also abundant products formed in about equal molar amounts, followed by
 261 smaller amounts of C₆ naphthenes. C₁₁ and traces of C₁₂ naphthenes (not represented) accounted
 262 altogether for less than 4% of this product fraction.

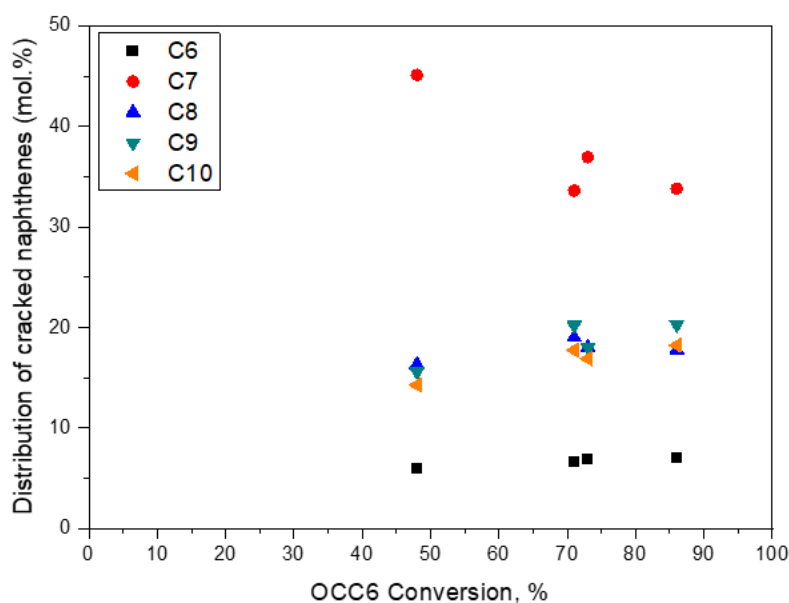


Figure 8. Distribution of cracked naphthenes as a function of octylcyclohexane conversion.

263 C₆ naphthenes (Figure 9A) were methylcyclopentane and cyclohexane. Methylcyclopentane
 264 was favored at all conversion levels over its 6-membered ring isomer. It reflects the
 265 thermodynamic equilibrium of these two isomers and the higher stability of
 266 methylcyclopentane at higher temperature⁵. Among the C₇ naphthenes (Figure 9B), the primary
 267 product was methylcyclohexane. The distribution then evolved towards the formation of
 268 dimethylcyclopentane. Ethylcyclopentane was a minority product in this fraction. This result
 269 differed from hydrocracking of perhydrophenanthrene⁵⁰ over the same catalyst, where in the C₇
 270 naphtene fraction the primary formation of the dibranched 5-membered naphthenic isomer was
 271 observed. This also confirms that the distribution of the naphthene cracking products was not
 272 an equilibrium distribution, but related to structure of the C₁₄ isomer, which undergoes cracking.

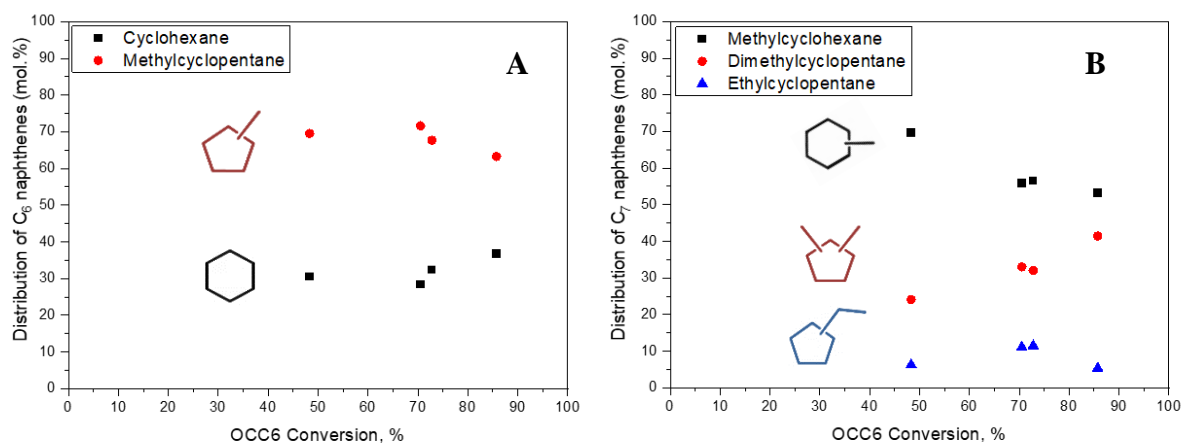


Figure 9. A) Distribution of C₆ naphthenes and B) Distribution of C₇ naphthenes as a function of octylcyclohexane conversion.

273 C₈ naphthenes comprised mono-, di- and tribranched structures (Figure 10). The most abundant
 274 isomer was dimethylcyclohexane; its proportion increased slightly with octylcyclohexane
 275 conversion. Unknown structures constituted about 10% of the distribution.

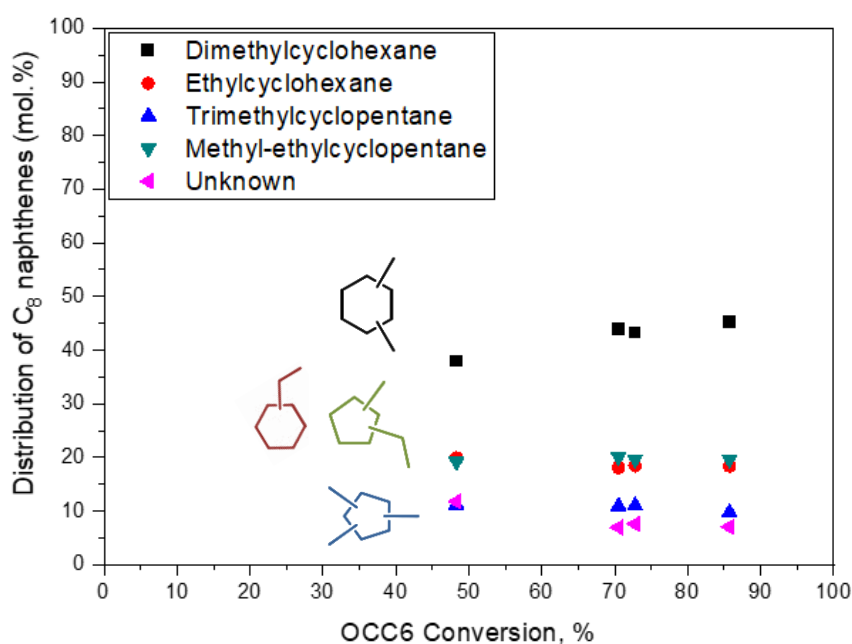


Figure 10. Distribution of C₈ naphthenes as a function of octylcyclohexane conversion.

276 The distribution of C₉ naphthenes is detailed in Figure 11. The most abundant cyclic C₉ isomers
 277 were di-branched (methyl-ethylcyclohexane, **C9-3**, and diethylcyclopentane, **C9-2**, which is a

278 ring contraction isomer of **C9-3**) or tri-branched (trimethyl-cyclohexane, **C9-1**). The
 279 distribution of C₉ naphthenes did not change significantly with octylcyclohexane conversion.
 280 Unknown compounds accounted for less than 5% of the distribution.

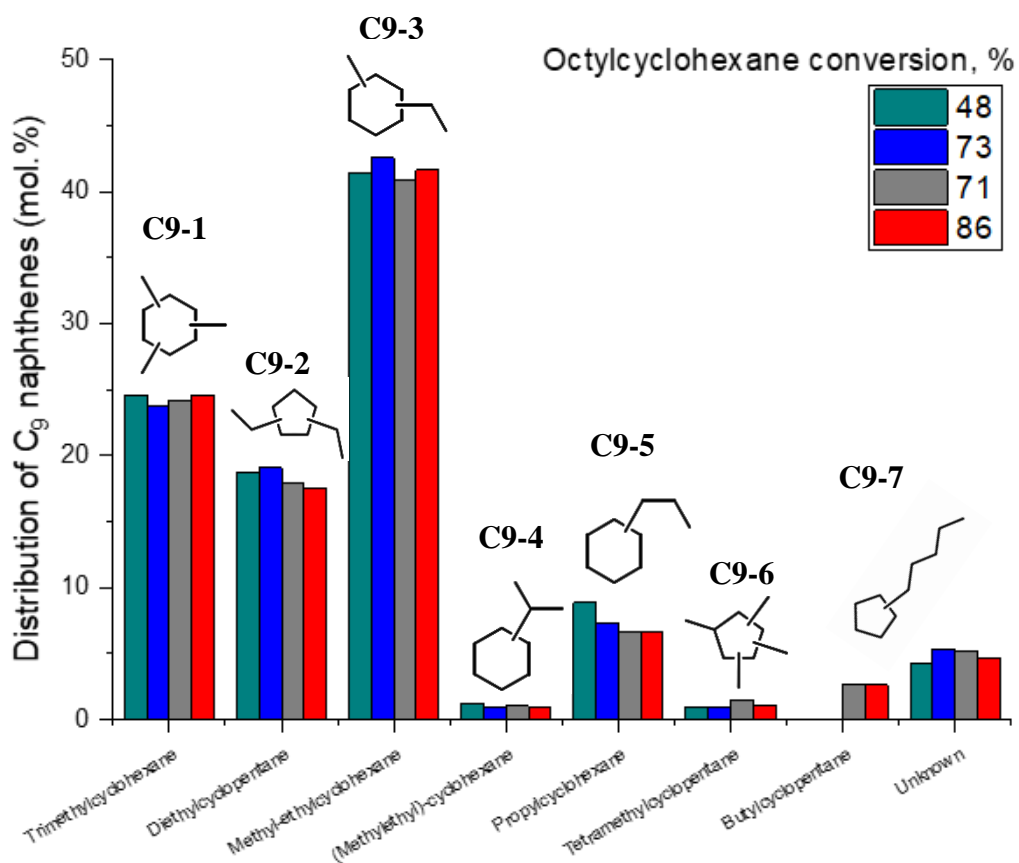


Figure 11. Distribution of C₉ naphthenes as a function of octylcyclohexane conversion.

281 In the C₁₀ naphthenes (Figure 12) the most abundant isomers were di-branched structures
 282 (diethyl, methyl-propyl substituted rings) and tribranched isomers (methyl-
 283 isopropylcyclohexane). 6-Ring structures dominated over 5-ring structures, like **C10-2**.
 284 Unknown molecules represented about 10% of the distribution.

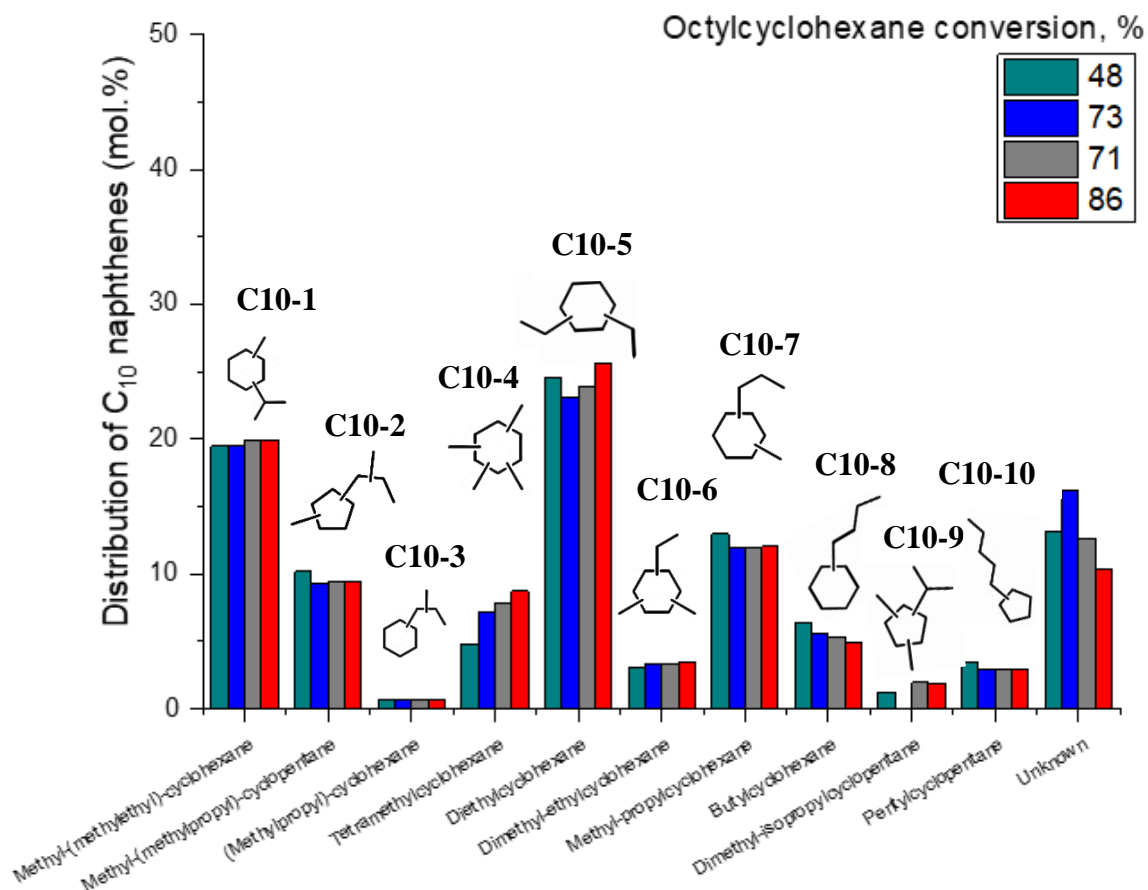


Figure 12. Distribution of C10 naphthenes as a function of octylcyclohexane conversion.

285 The distribution of iso- and n-alkanes in the carbon number fractions of cracked products is
 286 presented in Figure 13. The most abundant alkanes were C₄, C₅ and C₆ (the C₇ alkanes could
 287 not be distinguished from the solvent). Alkanes heavier than 8 carbon atoms were not formed.
 288 Isoalkanes were preferentially formed over linear isomers, they accounted for ca. 65 mol.% of
 289 the distribution.

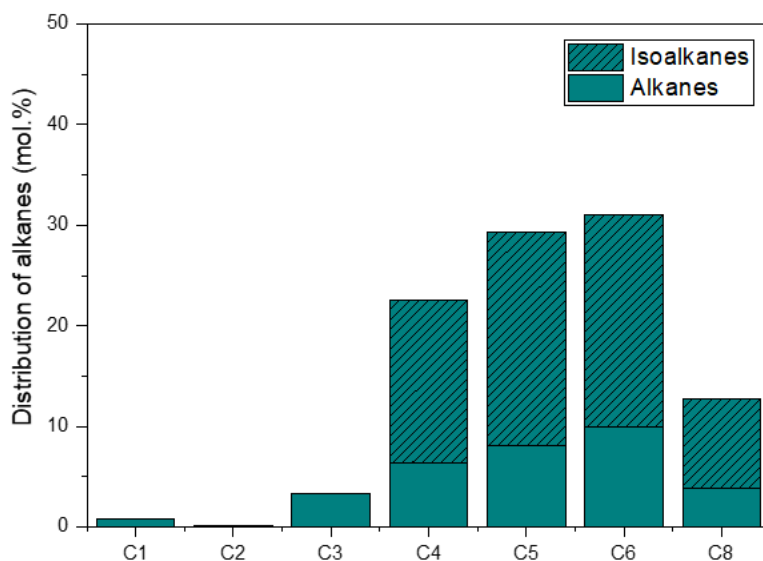


Figure 13. Molar composition of alkane cracked products at 48% octylcyclohexane conversion.

290 4 Discussion

291 4.1 Rationalization of isomerization pathways

292 A large variety of isomers was formed through hydroconversion of octylcyclohexane over Pt/H-
 293 USY zeolite catalyst (Figure 5). This diversity was reached by skeletal branching reactions,
 294 ring contraction and expansion, and alkyl-shifts. The branchiness of a molecule can be
 295 determined by counting tertiary C-atoms as one branching, and quaternary C-atoms as two. In
 296 carbocation chemistry, rearrangements which change the degree of branching, as type B
 297 rearrangements, should have a higher activation energy than alkyl-shifts, which only modify
 298 the position or type of branching (type A rearrangements). Naphthenes are particular because
 299 ring contractions (from 6-ring to 5-ring) also fall into the class of type A rearrangements
 300 although they introduce an additional branching on the formed 5-ring. In single events kinetic
 301 models of smaller model molecules^{45,60} the activation energy was estimated to obey the
 302 following order: alkyl shift on an aliphatic chain (exocyclic, type A) < alkyl shift on the ring
 303 (endocyclic, type A) << ring branching (type B) < chain branching (exocyclic, type B). Ring
 304 contractions/expansions can be considered as alkyl shifts on the ring.

305 According to this order, creation of branchings on the ring via ring contraction is faster than
 306 creation of branchings on the alkyl side chain. Branchings on the alkyl chain would not be
 307 generated directly, but originate from the transfer of alkyl groups from the ring to the chain⁴⁷.
 308 Here it was observed that only few of the C₁₄ isomers had branched alkyl-substituents. Having
 309 the knowledge from literature in mind, we will now discuss possible reaction pathways which
 310 could lead to the isomers observed in Figure 5.
 311 As already observed by Souverijns *et al.*⁴⁷, methyl-heptylcyclohexane (**I2**) is formed early on
 312 through ring-contraction of the reactant to methyl-octylcyclopentane (type B isomerization),
 313 followed by cycle expansion to form the 6-membered dibranched naphthene through type A
 314 isomerization (Figure 14). The content of methyl-heptylcyclohexane within the isomer family
 315 decreased slightly with conversion, suggesting that it was a primary isomerization product,
 316 which was then further converted to other isomers or cracked products.

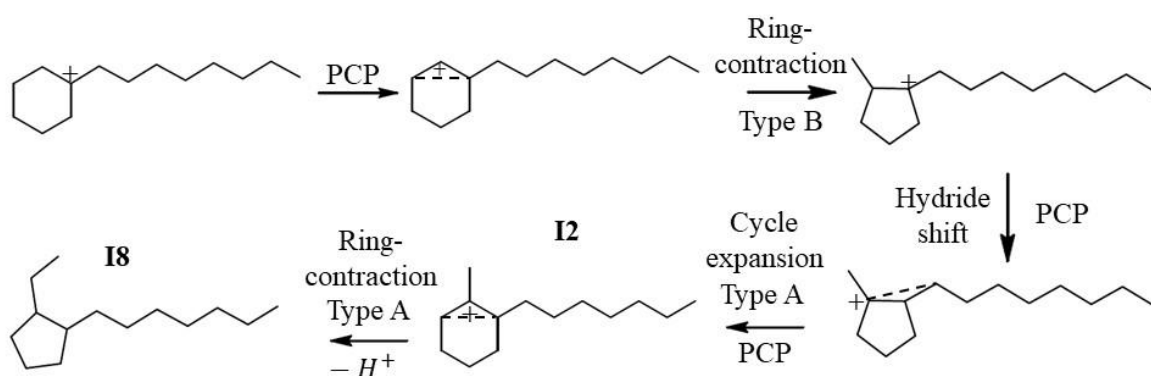
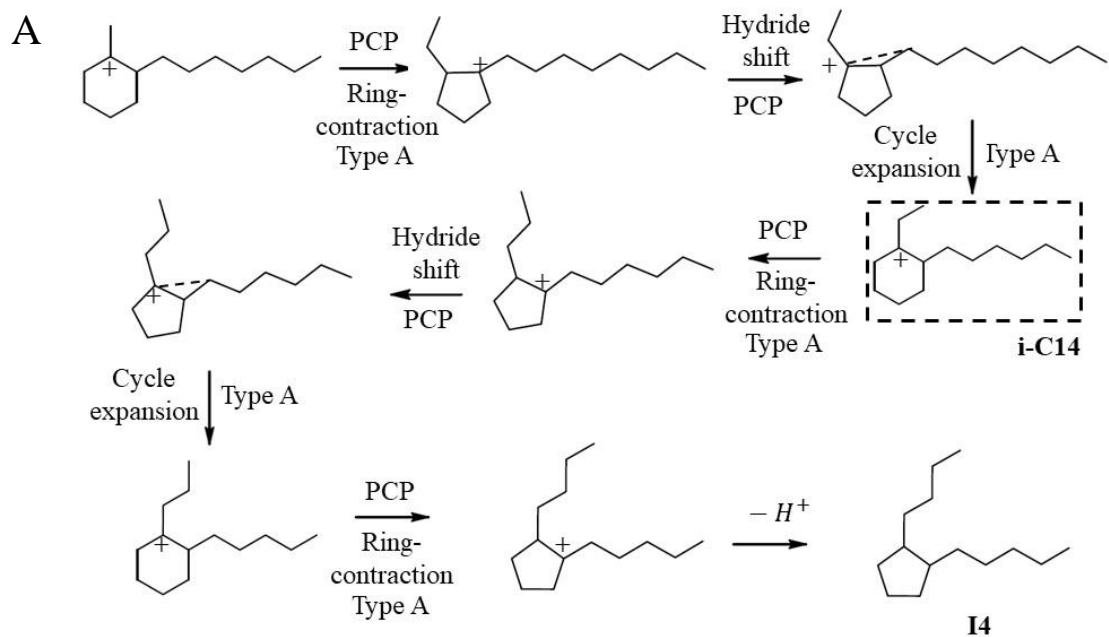


Figure 14. Suggested reaction pathway for isomerization of octylcyclohexane towards methyl-heptylcyclohexane (**I2**) and subsequently to ethyl-heptylcyclopentane (**I8**) over Pt/H-USY zeolite catalyst, in accordance with Souverijns *et al.*⁴⁷

317 Via a sequence of ring contraction and ring expansion steps (Figure 15A), **I2** can be transformed
 318 into the second most abundant isomer **I4** (via an ethyl-hexylcyclohexane intermediate i-C14).
 319 Since the degree of branching does not change going from **I2** to **I4**, the ring contraction and
 320 expansion steps are type A and should, therefore, be rather rapid. The formation of the third

321 most abundant isomer **I6** (tetrabranched) requires two type B ring contractions in order to add
 322 two additional branchings (Figure 15B), i.e. it is a more demanding pathway.



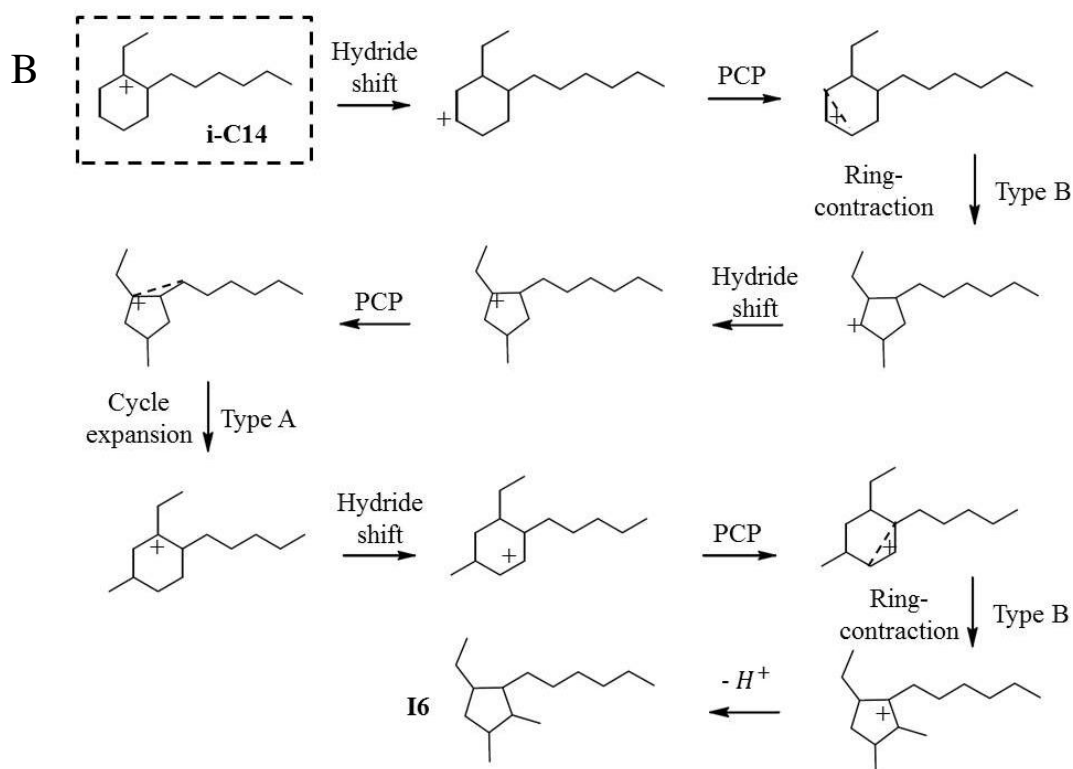


Figure 15. A) Suggested reaction pathway for isomerization of octylcyclohexane to isomer **I4** starting from methyl-heptylcyclohexane (**I2**). B) Suggested reaction pathway for isomerization of octylcyclohexane towards isomer **I6** starting from structure **i-C14**.

323 In general, the easiness to form a given isomer should be associated to the number of slow
 324 reaction steps needed for its formation. This approach provides us with a guideline to interpret
 325 the distribution of isomers presented in Figure 5. The number of branchings on cycle and on
 326 alkyl chains, as well as the total number of type B ring-contraction required to produce a specific
 327 isomer are presented in Table 1.

Table 1. Number of branchings on rings or on chains and type B ring-contraction required to produce isomers from octylcyclohexane over Pt/H-USY zeolite catalyst.

Isomer	Branchings on ring	Branchings on chains	Number of type B isomerization steps required for formation of isomer
I2	2	-	1
I4	2	-	1

I8	2	-	1
I7	3	-	2
I1	4	-	3
I6	4	-	3
I5	4	1	4
I3	4	2	5

328

329 According to Table 1, structures **I2**, **I4** and **I8** requiring only one type B isomerization are
330 expected to be formed early in the reaction network. **I2** and **I4** were indeed the dominating
331 isomers, but **I8** was formed in smaller amount. **I8** is formed by a type A ring contraction from
332 **I2** (Figure 14), the interconversion between the two molecules must be very easy. The low I8
333 yield is, therefore, tentatively attributed to a lower thermodynamic stability of this isomer.
334 Reaction pathways leading to structures **I7**, **I1** and **I6** involve one or two additional B type
335 isomerization steps, enhancing in this way the number of ring substituents. **I7** can be formed
336 by introducing an additional methyl branching in **I2**, by repeating the sequence of steps that
337 lead from octylcyclohexane to **I2**. We would expect the formation of **I7** to be kinetically favored
338 over **I6**, yet **I6** was more abundant. This is probably related to the suitability of **I7** for cracking
339 via beta-scission, which is less the case for **I6**, as will be discussed in the next section. Isomers
340 **I3** and **I5** involve more of such steps to generate branched alkyl groups on the ring. These highly
341 branched compounds were the least abundant in the isomer fraction, which correlates well to
342 the number of slow reactions steps involved in their formation.

343 4.2 Rationalization of hydrocracking pathways

344 Cracked products were formed in consecutive steps to isomerization and became predominant
345 around 70% octylcyclohexane conversion (Figure 4). The molar yield of cracked products was
346 close to 200 mol per 100 mol feed molecules cracked (Figure 6). These values correspond

347 globally to cracking of one molecule into two other ones, as expected for a single cracking
348 event. This contrasts with the hydrocracking of perhydrophenanthrene, a polycyclic naphthene
349 with 14 C-atoms, where the analysis of the yield of cracked products revealed values below 200
350 mol per 100 mol cracked, indicating an important contribution of oligomerization-cracking
351 mechanisms⁵⁰.

352 The molar yield of cracked products (Figure 6) shows a predominant cracking to C₇, and since
353 for reasons already explained C₇ alkanes are not included, the dominance of this fraction is most
354 probably even higher. Molar yields of fractions with 4 to 10 C-atoms are about equal. The C₄
355 fraction does not contain naphthenes. C₅ and C₆ products were mainly iso-alkanes, while C₈ to
356 C₁₀ products were mainly naphthenes. This suggests a cracking of a C₁₄ isomer to a C_n alkane
357 and a C_{14-n} naphthene, n ranging in majority from 4 to 7. The absence of secondary cracking
358 finds an explanation in this product distribution. C₄ and C₅ molecules do not undergo much
359 hydrocracking, because no favorable beta-scission mechanisms are available. Beta-scission
360 would involve primary alkylcarbenium ions. C₆ and C₇ alkanes are more sensitive to
361 hydrocracking, but at least 8 C-atoms in an alkane are needed to enable hydrocracking via the
362 fast beta-scission pathway converting a tertiary alkylcarbenium ion to a smaller alkylcarbenium
363 ion and an olefin⁴⁴.

364 Given the dominancy of primary cracking, the main pathway leads to the formation of C₇
365 naphthenes and C₇ alkanes. The distribution of C₇ naphthenes depicted in Figure 9B indicated
366 a primary formation of methylcyclohexane. We further suppose that the C₇ alkane was an iso-
367 alkane, i.e. the sum of branchings in the cracking products was two. Since cracking reduces the
368 degree of branching by one unit, the reactant isomer must have been tri-branched, i.e. **I7**. As
369 shown in Figure 16, **I7** can indeed readily crack into methyl-cyclohexane and methylhexane
370 after shifting a methyl substituent from the ring to the chain. The readiness of long branched
371 side-chains to crack may also explain why such long branched alkyl-substituents were not

372 detected among the isomers. In earlier work on octylcyclohexane isomerization at lower
 373 conversion levels, such isomers had been observed.⁴⁷

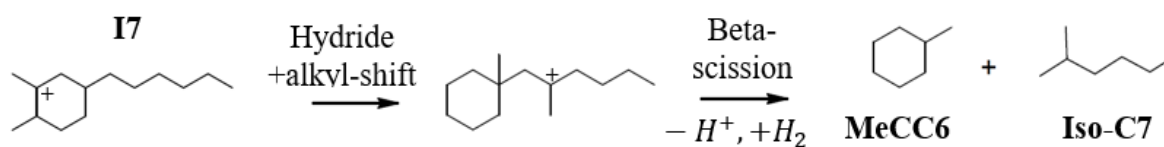


Figure 16. Suggested cracking pathway towards formation of methylcyclohexane and methylhexane from hydrocracking of **I7** isomer.

374
 375 The hydrocracking to C₈ naphthenes and a C₆ alkane can be analyzed in a same way. The
 376 dominant C₆ isoalkane was 2-methylpentane, and the primary C₈ naphthenes were
 377 dimethylcyclohexanes, methyl-ethylcyclopentanes and ethylcyclohexanes (Figure 10). Hence,
 378 the reactant isomer must have been at least tetra- or tri-branched. Among the tetrabranched
 379 isomers which were observed (**I1** and **I6**), only **I6** is suited for cracking into a C₆ alkane. A
 380 possible reaction pathway is shown in Figure 17. It only requires an alkyl shift from the ring to
 381 the chain in order to allow a favorable beta scission. The methyl-ethylcyclopentane product can
 382 easily convert to dimethylcyclohexane (the major C₈ naphthene) by type A ring expansion.
 383 Also the tri-branched **I7** isomer can crack to ethylcyclohexane and isohexane, after methyl shift
 384 to the long alkyl chain and type A ring-contraction/expansion in order to redistribute the length
 385 of the alkyl substituents (not shown).

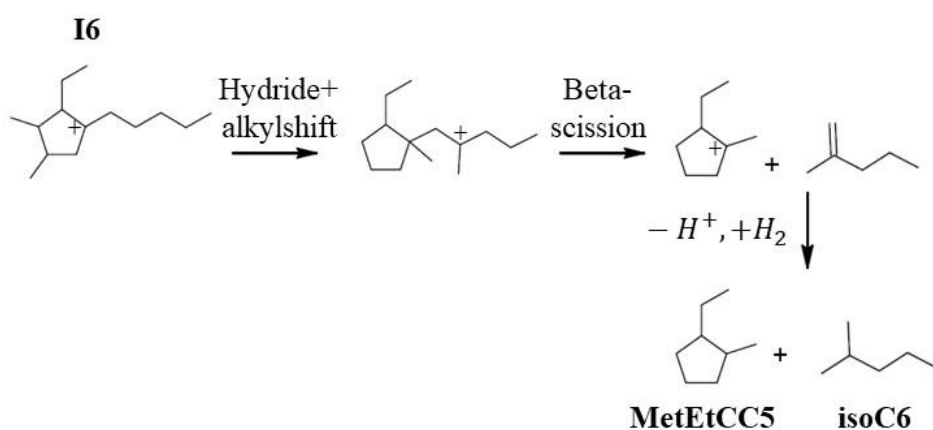


Figure 17. Suggested cracking pathway towards formation of methyl-ethylcyclopentane and methylpentane from hydrocracking of **I6** isomer.

386

387 The **I6** isomer can crack to C₈ + C₆, but also C₉ + C₅. For this **I6** has to undergo cycle expansion
 388 and an alkyl shift from ring to chain. The resulting intermediate can readily crack to di-branched
 389 C₉ naphthenes (in line with Figure 11) and iso-pentane (Figure 18).

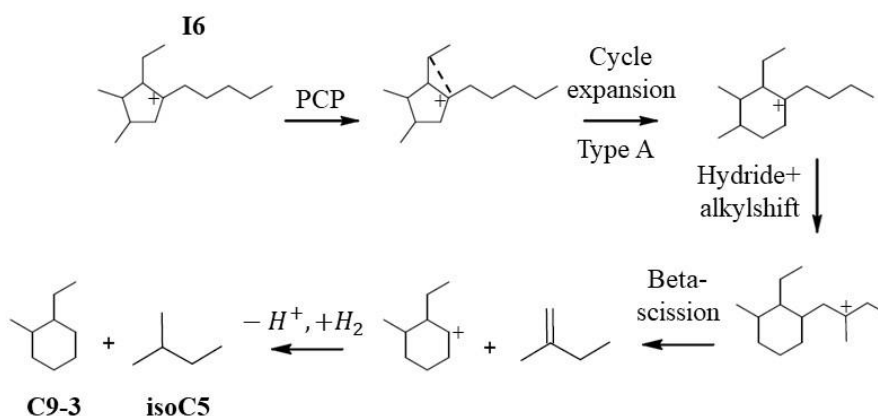


Figure 18. Suggested cracking pathway towards formation of structure **C9-3** and methylbutane from hydrocracking of **I6** isomer.

390

391 Another possible pathway is cracking of C₁₄H₂₈ isomers into C₁₀ naphthenes and C₄ alkanes.
 392 C₁₀ compounds and comprised especially of diethylcyclohexane (**C10-5**, dibranched) and
 393 methyl-isopropylcyclohexane (**C10-1**, tribranched) (Figure 12). This implies that the parent
 394 isomers cracked to these C₁₀ naphthenes contained at least four branchings. The **I6** molecule
 395 can crack to di-branched C₁₀ naphthenes, but compared to the schemes shown above, this
 396 pathway requires additional A ring-contraction and expansion reactions. **I5**-type structures can
 397 undergo hydrocracking to tri-branched products within the C₁₀ naphthenes fraction after a small
 398 number of type A rearrangements, because an isobutyl group is already attached to the
 399 naphthenic cycle (Figure 19).

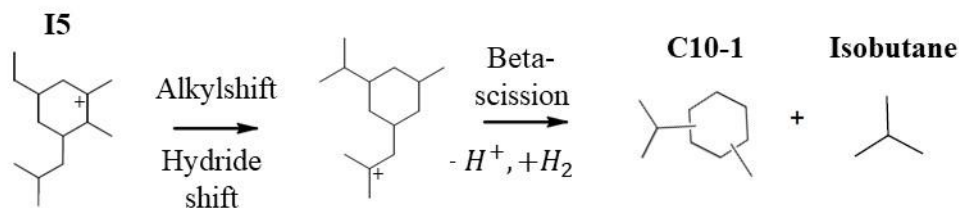


Figure 19. Suggested cracking pathway towards formation of structure C10-1 and isobutane from hydrocracking of **I5** isomer.

400

401 Structures **I1** and **I3** present short side chains and would have to isomerize multiple times to

402 generate a longer side chain (via type A and B rearrangements), which could favorably crack

403 to C₁₀ naphthenes and isobutane. The formation of **I1** and **I3** can, therefore, be considered as a

404 dead end route.

405 The above analysis of reaction pathways can be summarized in the reaction scheme shown in

406 Figure 20. The reactant first isomerized to methyl-heptylcyclohexane (**I2**). **I2** can easily

407 rearrange to other di-branched structures (**I4**) or create an additional branching on the ring and

408 form **I7**. **I7** can either crack to two C₇ fragments or isomerize further to **I6** and eventually **I5**.

409 The cracking of **I6** and **I5** explains the formation of C₈ + C₆, C₉ + C₅ and C₁₀ + C₄ products.

410 Further isomerization leads to structures with shorter side chains, which cannot crack (**I1** and

411 **I3**).

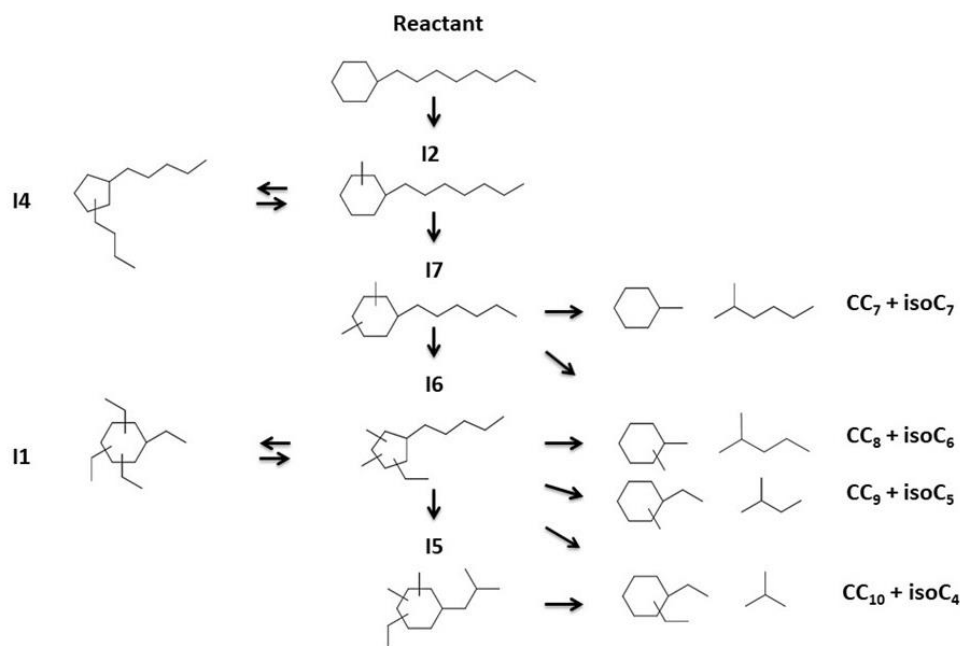


Figure 20. Main reaction pathways in the hydroconversion of octylcyclohexane.

412

413 Based on the general reaction scheme (Figure 20), an attempt can be made to rationalize the
 414 carbon number distribution of the cracked products (Figure 6). The peak for C₇ compounds
 415 suggests that the cracking of the **I7** intermediate is a very favorable reaction pathway, which
 416 successfully competes with further isomerization to more highly branched structures. It shows
 417 that long alkyl side chains are ready to crack once the minimum branching required to reach a
 418 favorable cracking configuration has been attained.

419 It is more difficult to explain why the other cracking products, i.e. C₈, C₉ and C₁₀ naphthenes,
 420 are formed in almost equimolar amounts (Figure 6), although they may be formed from
 421 different isomers (**I7**, **I6**, **I5**), which do not have the same abundance. A more detailed kinetic
 422 investigation would be required to answer that question.

423 Striking is that the carbon number distribution in the cracked products strongly deviates from
 424 the ones that were reported for the classical paring reaction, i.e. a peak for isobutane
 425 accompanied by a peak for the C_{n-4} naphthene⁴². The reason for this discrepancy probably lies

426 in the nature of the reactant. The previous studies were carried out with highly substituted
427 cyclohexane rings with very short side chains. These reactants have to undergo isomerization
428 steps in order to form at least an isobutyl side chain, which is the first one that allows favorable
429 cracking. Cracking to isobutane is, therefore, observed as the major reaction pathway in the
430 paring reaction. In the present case, we started from a long alkyl chain; after introducing the
431 minimum number of required branchings on the naphthene ring by shifting some carbon atoms
432 to newly generated side chains, what is remaining of the original alkyl chain is still quite long
433 and susceptible to cracking. Starting from a C₈ side chain, dealkylation of that chain leads to
434 the formation of C₇ alkanes, and depending of the number of such shifts of carbon atoms, to C₆,
435 C₅ and C₄. Expressed in a different way: long alkyl substituents on a naphthene ring can readily
436 undergo cracking to long alkyl chains (and a pared naphthene), provided that three branchings
437 are present in the molecule.

438 5 Conclusions

439 Hydroisomerization of octylcyclohexane over the bifunctional Pt/USY catalyst results in a
440 variety of isomerization products, presenting from 2 to 6 branchings. Cracked products appear
441 as secondary products and become predominant at average conversion, while ring-opening
442 products were hardly formed on the investigated zeolite catalyst.

443 Hydroconversion of octylcyclohexane over Pt/USY zeolite catalyst starts via the formation of
444 di-branched products, i.e. mainly methyl-heptyl substituted cyclohexane. These di-branched
445 naphthenes do not seem to crack, but they isomerize further to tri-branched isomers. Tri-
446 branched isomers have the possibility to crack favorably into a mono-branched C₇ naphthene
447 and a C₇ iso-alkane. This is the dominant reaction pathway.

448 The cracking of the tri-branched isomer competes with its further isomerization to more highly
449 branched isomers. The more highly branched isomers have shorter alkyl side chains and the
450 remainder of the long chain cracks to C₆, C₅ or C₄ (iso-)alkanes and the corresponding

451 naphthene having methyl or ethyl substituents. Highly branched isomerization products with
452 very short side chain cannot crack favorably and can, therefore, be considered as refractory
453 isomers.

454 This mechanistic insight explains why the hydrocracking of this C₁₄-naphthene with a long
455 alkyl side chain (C₈) leads to a peak at 7 C-atoms in the carbon number distribution of the
456 cracking products and otherwise a fairly flat distribution ranging from 4 to 10 carbon atoms.
457 This differs from the typical bimodal distributions observed with smaller naphthenes, which
458 react according to the paring reaction leading to isobutane as main alkane product. A typical
459 cracked product distribution obtained by the paring reaction shows a maximum at C₄ and
460 another one at C_{n-4}. Our work shows that such bimodal product distribution will not be obtained
461 in the cracking of naphthenes with long alkyl substituents, because they readily crack to longer
462 alkyl chains according to the mechanism explained above. These insights provide a guide for
463 interpreting the carbon number distributions obtained in the hydrocracking of heavy feeds, like
464 VGO, where naphthenes with long alkyl substituents are frequently encountered.

465 **Acknowledgment**

466 J. Martens acknowledges the Flemish Government for long term structural funding
467 (Methusalem program).

468 **6 References**

469 (1) Viswanathan, B. Chapter 2 - Petroleum. In *Energy Sources*; Viswanathan, B., Ed.; Elsevier,
470 2017; pp 29–57. DOI: 10.1016/B978-0-444-56353-8.00002-2.

471 (2) Speight, J. G. Thermal Decomposition of Hydrocarbons. In *Handbook of industrial*
472 *hydrocarbon processes*, First edition; Speight, J. G., Ed.; Elsevier/Gulf Professional Publishing,
473 Amsterdam, Boston, 2011; pp 395–428. DOI: 10.1016/B978-0-7506-8632-7.10011-8.

- 474 (3) Sahu, R.; Song, B. J.; Im, J. S.; Jeon, Y.-P.; Lee, C. W. A review of recent advances in
475 catalytic hydrocracking of heavy residues. *J. Ind. Eng. Chem.* **2015**, *27*, 12–24. DOI:
476 10.1016/j.jiec.2015.01.011.
- 477 (4) Scherzer, J.; Gruia, A. J. *Hydrocracking science and technology*; Chemical industries, Vol.
478 66; M. Dekker, New York, 1996.
- 479 (5) Marcilly, C. *Acido-basic catalysis*; IFP publications, Ed. Technip, Paris, 2005.
- 480 (6) Bertoncini, F.; Bonduelle, A.; Francis, J.; Guillon, E. Hydrocracking. In *Catalysis by*
481 *Transition Metal Sulfides*; Toulhoat, H., Raybaud, P., Eds.; Ed. Technip, Paris, 2013; p 609.
- 482 (7) Altgelt, K. H.; Boduszynski, M. M. *Composition and analysis of heavy petroleum fractions*;
483 Marcel Dekker, New York, 1993.
- 484 (8) Dutriez, T. Chromatographie multidimensionnelle : vers une caractérisation moléculaire
485 étendue des charges type distillat sous vide et la compréhension de leur réactivité à
486 l'hydrotraitement, Doctoral Thesis, Université Pierre et Marie Curie, Paris, 2010.
- 487 (9) Alvarez, F.; Ribeiro, F. R.; Perot, G.; Thomazeau, C.; Guisnet, M. Hydroisomerization and
488 Hydrocracking of Alkanes. *J. Catal.* **1996**, *162* (2), 179–189. DOI: 10.1006/jcat.1996.0275.
- 489 (10) Calemma, V.; Peratello, S.; Perego, C. Hydroisomerization and hydrocracking of long
490 chain n-alkanes on Pt/amorphous SiO₂–Al₂O₃ catalyst. *Appl. Catal. A* **2000**, *190* (1-2), 207–
491 218. DOI: 10.1016/S0926-860X(99)00292-6.
- 492 (11) Claude, M. C.; Vanbutsele, G.; Martens, J. A. Dimethyl Branching of Long n-Alkanes in
493 the Range from Decane to Tetracosane on Pt/H–ZSM-22 Bifunctional Catalyst. *J. Catal.* **2001**,
494 *203* (1), 213–231. DOI: 10.1006/jcat.2001.3325.
- 495 (12) J. Weitkamp; Jacobs, P. A.; Martens, J. A. Isomerization and hydrocracking of C₉ through
496 C₁₆ n-alkanes on Pt/HZSM-5 zeolite. *Appl. Catal.* **1983**, *8*, 123–141.

- 497 (13) Bi, Y.; Xia, G.; Huang, W.; Nie, H. Hydroisomerization of long chain n-paraffins: The role
498 of the acidity of the zeolite. *RSC Adv.* **2015**, *5* (120), 99201–99206. DOI:
499 10.1039/C5RA13784E.
- 500 (14) Noh, G.; Shi, Z.; Zones, S. I.; Iglesia, E. Isomerization and β -scission reactions of alkanes
501 on bifunctional metal-acid catalysts: Consequences of confinement and diffusional constraints
502 on reactivity and selectivity. *J. Catal.* **2018**, *368*, 389–410. DOI: 10.1016/j.jcat.2018.03.033.
- 503 (15) Jacobs, P. A.; Martens, J. A. Chapter 12 Introduction to Acid Catalysis with Zeolites in
504 Hydrocarbon Reactions. In *Introduction to zeolite science and practice*; van Bekkum, H.,
505 Flanigen, E. M., Jansen, J. C., Eds.; Studies in Surface Science and Catalysis; Elsevier, 1991;
506 pp 445–496. DOI: 10.1016/S0167-2991(08)63610-1.
- 507 (16) Burnens, G.; Bouchy, C.; Guillon, E.; Martens, J. A. Hydrocracking reaction pathways of
508 2,6,10,14-tetramethylpentadecane model molecule on bifunctional silica–alumina and
509 ultrastable Y zeolite catalysts. *J. Catal.* **2011**, *282* (1), 145–154. DOI:
510 10.1016/j.jcat.2011.06.007.
- 511 (17) Valéry, E.; Guillaume, D.; Surla, K.; Galtier, P.; Verstraete, J.; Schweich, D. Kinetic
512 Modeling of Acid Catalyzed Hydrocracking of Heavy Molecules: Application to Squalane. *Ind.*
513 *Eng. Chem. Res.* **2007**, *46* (14), 4755–4763. DOI: 10.1021/ie061559w.
- 514 (18) Arribas, M. A.; Martínez, A.; Sastre, G. Simultaneous hydrogenation and ring opening of
515 aromatics for diesel upgrading on Pt/zeolite catalysts. The influence of zeolite pore topology
516 and reactant on catalyst performance. In *Impact of zeolites and other porous materials on the*
517 *new technologies at the beginning of the new millennium: Proceedings of the 2nd International*
518 *FEZA (Federation of the European Zeolite Associations) Conference, Taormina, Italy,*
519 *September 1-5, 2002*, 1st ed.; Aiello, R., Giordano, G., Testa, F., Eds.; Studies in Surface
520 Science and Catalysis, Vol. 142; Elsevier, 2002; pp 1015–1022. DOI: 10.1016/S0167-
521 2991(02)80258-0.

- 522 (19) Arribas, M. A.; Concepción, P.; Martínez, A. The role of metal sites during the coupled
523 hydrogenation and ring opening of tetralin on bifunctional Pt(Ir)/USY catalysts. *Appl. Catal. A*
524 **2004**, 267 (1-2), 111–119. DOI: 10.1016/j.apcata.2004.02.037.
- 525 (20) Bellussi, G.; Haas, A.; Rabl, S.; Santi, D.; Ferrari, M.; Calemma, V.; Weitkamp, J.
526 Catalytic Ring Opening of Perhydroindan – Hydrogenolytic and Cationic Reaction Paths. *Chin.*
527 *J. Catal.* **2012**, 33 (1), 70–84. DOI: 10.1016/S1872-2067(10)60278-1.
- 528 (21) Blanco, E.; Piccolo, L.; Laurenti, D.; Di Felice, L.; Catherin, N.; Lorentz, C.; Geantet, C.;
529 Calemma, V. Effect of H₂S on the mechanisms of naphthene ring opening and isomerization
530 over Ir/NaY:A comparative study of decalin, perhydroindan and butylcyclohexane
531 hydroconversions. *Appl. Catal. A* **2018**, 550, 274–283. DOI: 10.1016/j.apcata.2017.11.020.
- 532 (22) Calemma, V.; Ferrari, M.; Rabl, S.; Weitkamp, J. Selective ring opening of
533 naphthenes: From mechanistic studies with a model feed to the upgrading of a hydrotreated light
534 cycle oil. *Fuel* **2013**, 111, 763–770. DOI: 10.1016/j.fuel.2013.04.055.
- 535 (23) Catherin, N.; Blanco, E.; Piccolo, L.; Laurenti, D.; Simonet, F.; Lorentz, C.; Leclerc, E.;
536 Calemma, V.; Geantet, C. Selective ring opening of decalin over bifunctional RuS₂/zeolite
537 catalysts. *Catal. Today* **2019**, 323, 105–111. DOI: 10.1016/j.cattod.2018.07.052.
- 538 (24) Di Felice, L.; Catherin, N.; Piccolo, L.; Laurenti, D.; Blanco, E.; Leclerc, E.; Geantet, C.;
539 Calemma, V. Decalin ring opening over NiWS/SiO₂-Al₂O₃ catalysts in the presence of H₂
540 S. *Appl. Catal. A* **2016**, 512, 43–51. DOI: 10.1016/j.apcata.2015.12.007.
- 541 (25) Du, H.; Fairbridge, C.; Yang, H.; Ring, Z. The chemistry of selective ring-opening
542 catalysts. *Appl. Catal. A* **2005**, 294 (1), 1–21. DOI: 10.1016/j.apcata.2005.06.033.
- 543 (26) Haas, A. Ring Opening of Mono- and Bicyclic Naphthenes via Hydrogenolysis on Noble
544 Metal Catalysts, Doctoral Thesis, University of Stuttgart, 2012.

545 (27) Holl, T. Competitive Hydroconversion of Decalin and n-Decane on Noble-Metal Catalysts
546 and the Evaluation of Molybdenum Carbide as Ring-Opening Catalyst, Doctoral Thesis,
547 University of Stuttgart, 2014. <http://dx.doi.org/10.18419/opus-1409>.

548 (28) Piccolo, L.; Nassreddine, S.; Toussaint, G.; Geantet, C. Mechanism of tetralin ring
549 opening and contraction over bifunctional Ir/SiO₂-Al₂O₃ Catalysts. *ChemSusChem* **2012**, *5* (9),
550 1717–1723. DOI: 10.1002/cssc.201200080.

551 (29) Rabl, S.; Santi, D.; Haas, A.; Ferrari, M.; Calemma, V.; Bellussi, G.; Weitkamp, J.
552 Catalytic ring opening of decalin on Ir- and Pt-containing zeolite Y – Influence of the nature of
553 the charge-compensating alkali cations. *Microporous Mesoporous Mater.* **2011**, *146* (1-3),
554 190–200. DOI: 10.1016/j.micromeso.2011.03.045.

555 (30) Santi, D.; Holl, T.; Calemma, V.; Weitkamp, J. High-performance ring-opening catalysts
556 based on iridium-containing zeolite Beta in the hydroconversion of decalin. *Appl. Catal. A*
557 **2013**, *455*, 46–57. DOI: 10.1016/j.apcata.2013.01.020.

558 (31) Martínez, A.; Arribas, M. A.; Pergher, S. B. C. Bifunctional noble metal/zeolite catalysts
559 for upgrading low-quality diesel fractions via selective opening of naphthenic rings. *Catal. Sci.*
560 *Technol.* **2016**, *6* (8), 2528–2542. DOI: 10.1039/C6CY00135A.

561 (32) Benazzi, E.; Leite, L.; Marchal-George, N.; Toulhoat, H.; Raybaud, P. New insights into
562 parameters controlling the selectivity in hydrocracking reactions. *J. Catal.* **2003**, *217* (2), 376–
563 387. DOI: 10.1016/S0021-9517(03)00041-1.

564 (33) Leite, L.; Benazzi, E.; Marchal-George, N. Hydrocracking of phenanthrene over
565 bifunctional Pt catalysts. *Catal. Today* **2001**, *65*, 241–247.

566 (34) Lee, S.-U.; Lee, Y.-J.; Kim, J.-R.; Kim, E.-S.; Kim, T.-W.; Kim, H. J.; Kim, C.-U.; Jeong,
567 S.-Y. Selective ring opening of phenanthrene over NiW-supported mesoporous HY zeolite
568 catalyst depending on their mesoporosity. *Mater. Res. Bull.* **2017**, *96*, 149–154. DOI:
569 10.1016/j.materresbull.2017.05.002.

- 570 (35) Martinez-Saavedra, J.-M.; Tavera-Mendez, C.-L.; Sandoval-Diaz, L.-E.; Pérez-Martínez,
571 D. d. J.; Rodríguez-Niño, G.; Trujillo, C.-A. Fluorene hydrocracking over bifunctional platinum
572 catalysts in a high-pressure simultaneous thermal analyzer. *Appl. Catal. A* **2021**, *616*, 118097.
573 DOI: 10.1016/j.apcata.2021.118097.
- 574 (36) Kubička, D.; Kumar, N.; Mäki-Arvela, P.; Venäläinen, T.; Tiitta, M.; Salmi, T.; Murzin,
575 D. Ring opening of decalin over Pt-and Ir-modified SAPO-5 and VPI-5 zeolite catalysts. In
576 *Molecular sieves: From basic research to industrial applications : Proceedings of the 3rd*
577 *International zeolite symposium : Prague, Czech Republic, August 23-26, 2005*; Studies in
578 Surface Science and Catalysis, Vol. 158; Elsevier, op. 2005; pp 1669–1676. DOI:
579 10.1016/S0167-2991(05)80524-5.
- 580 (37) Kubička, D.; Kumar, N.; Mäki-Arvela, P.; Tiitta, M.; Niemi, V.; Karhu, H.; Salmi, T.;
581 Murzin, D. Y. Ring opening of decalin over zeolitesII. Activity and selectivity of platinum-
582 modified zeolites. *J. Catal.* **2004**, *227* (2), 313–327. DOI: 10.1016/j.jcat.2004.07.015.
- 583 (38) Kubička, D.; Salmi, T.; Tiitta, M.; Murzin, D. Y. Ring-opening of decalin – Kinetic
584 modelling. *Fuel* **2009**, *88* (2), 366–373. DOI: 10.1016/j.fuel.2008.09.004.
- 585 (39) Monteiro, C. A.; Costa, D.; Zotin, J. L.; Cardoso, D. Effect of metal–acid site balance on
586 hydroconversion of decalin over Pt/Beta zeolite bifunctional catalysts. *Fuel* **2015**, *160*, 71–79.
587 DOI: 10.1016/j.fuel.2015.07.054.
- 588 (40) Oliveira Soares, L. W.; Castellã Pergher, S. B. Influence of the Brønsted Acidity on the
589 Ring Opening of Decalin for Pt-USY Catalysts. *Catalysts* **2019**, *9* (10), 786. DOI:
590 10.3390/catal9100786.
- 591 (41) Abbot, J. Active sites and intermediates for isomerization and cracking of cyclohexane on
592 HY. *J. Catal.* **1990**, *123*, 383–395.

- 593 (42) Egan, C. J.; Langlois, G. E.; White, R. J. Selective Hydrocracking of C 9 - to C 12 -
594 Alkylcyclohexanes on Acidic Catalysts. Evidence for the Paring Reaction. *J. Am. Chem. Soc.*
595 **1962**, *84* (7), 1204–1212. DOI: 10.1021/ja00866a028.
- 596 (43) Weitkamp, J.; Ernst, S.; Karge, H. G. Peculiarities in the conversion of naphthenes on
597 bifunctional catalysts. *Erdöl & Kohle, Erdgas, Petrochemie*. **1984**, *37*.
- 598 (44) Weitkamp, J. Catalytic Hydrocracking-Mechanisms and Versatility of the Process.
599 *ChemCatChem* **2012**, *4* (3), 292–306. DOI: 10.1002/cctc.201100315.
- 600 (45) Martens, G. G.; Thybaut, J. W.; Marin, G. B. Single-Event Rate Parameters for the
601 Hydrocracking of Cycloalkanes on Pt/US-Y Zeolites. *Ind. Eng. Chem. Res.* **2001**, *40* (8), 1832–
602 1844. DOI: 10.1021/ie000799n.
- 603 (46) Brouwer, D. M.; Hogeveen, H. *Recl. Trav. Chim. Pays-Bas* **1970**, *89*, 211–224.
- 604 (47) Souverijns, W.; Parton, R.; Martens, J. A.; Froment, G. F.; Jacobs, P. A. Mechanism of
605 the paring reaction of naphtenes. *Catal. Lett.* **1996**, *37* (3-4), 207–212. DOI:
606 10.1007/BF00807755.
- 607 (48) Dutriez, T.; Courtiade, M.; Thiébaud, D.; Dulot, H.; Bertoncini, F.; Vial, J.; Hennion, M.-
608 C. High-temperature two-dimensional gas chromatography of hydrocarbons up to nC60 for
609 analysis of vacuum gas oils. *Journal of chromatography. A* **2009**, *1216* (14), 2905–2912. DOI:
610 10.1016/j.chroma.2008.11.065.
- 611 (49) Dutriez, T.; Courtiade, M.; Thiébaud, D.; Dulot, H.; Hennion, M.-C. Improved
612 hydrocarbons analysis of heavy petroleum fractions by high temperature comprehensive two-
613 dimensional gas chromatography. *Fuel* **2010**, *89* (9), 2338–2345. DOI:
614 10.1016/j.fuel.2009.11.041.
- 615 (50) Brito, L.; Pirngruber, G. D.; Guillon, E.; Albrieux, F.; Martens, J. A. Hydroconversion of
616 perhydrophenanthrene over bifunctional Pt/H-USY zeolite catalyst. *ChemCatChem* **2020**, *12*,
617 3477–3488. DOI: 10.1002/cctc.201902372.

- 618 (51) Zečević, J.; Vanbutsele, G.; Jong, K. P. de; Martens, J. A. Nanoscale intimacy in
619 bifunctional catalysts for selective conversion of hydrocarbons. *Nature* **2015**, *528* (7581), 245–
620 248. DOI: 10.1038/nature16173.
- 621 (52) Oenema, J.; Harmel, J.; Vélez, R. P.; Meijerink, M. J.; Eijsvogel, W.; Poursaeidesfahani,
622 A.; Vlugt, T. J. H.; Zečević, J.; Jong, K. P. de. Influence of Nanoscale Intimacy and Zeolite
623 Micropore Size on the Performance of Bifunctional Catalysts for n-Heptane
624 Hydroisomerization. *ACS Catal.* **2020**, *10* (23), 14245–14257. DOI: 10.1021/acscatal.0c03138.
625 Published Online: Nov. 21, 2020.
- 626 (53) van der Wal, L. I.; Oenema, J.; Smulders, L. C. J.; Samplonius, N. J.; Nandpersad, K. R.;
627 Zečević, J.; Jong, K. P. de. Control and Impact of Metal Loading Heterogeneities at the
628 Nanoscale on the Performance of Pt/Zeolite Y Catalysts for Alkane Hydroconversion. *ACS*
629 *Catal.* **2021**, *11* (7), 3842–3855. DOI: 10.1021/acscatal.1c00211. Published Online: Mar. 12,
630 2021.
- 631 (54) Cheng, K.; van der Wal, L. I.; Yoshida, H.; Oenema, J.; Harmel, J.; Zhang, Z.; Sunley,
632 G.; Zečević, J.; Jong, K. P. de. Impact of the Spatial Organization of Bifunctional Metal-Zeolite
633 Catalysts on the Hydroisomerization of Light Alkanes. *Angew. Chem. Int. Ed.* **2020**, *59* (9),
634 3592–3600. DOI: 10.1002/anie.201915080.
- 635 (55) Mendes, P. S. F.; Silva, J. M.; Ribeiro, M. F.; Daudin, A.; Bouchy, C. Bifunctional
636 Intimacy and its Interplay with Metal-Acid Balance in Shaped Hydroisomerization Catalysts.
637 *ChemCatChem* **2020**, *12* (18), 4582–4592. DOI: 10.1002/cctc.202000624.
- 638 (56) Pirngruber, G. D.; Maury, S.; Daudin, A.; Alspektor, P. Y.; Bouchy, C.; Guillon, E.
639 Balance between (De)hydrogenation and Acid Sites: Comparison between Sulfide-Based and
640 Pt-Based Bifunctional Hydrocracking Catalysts. *Ind. Eng. Chem. Res.* **2020**, *59* (28), 12686–
641 12695. DOI: 10.1021/acs.iecr.0c01680.

642 (57) Brito, L. Hydroisomerization and hydrocracking of naphthenes, Doctoral Thesis,
643 Université Lyon 1, 2020. <http://www.theses.fr/2020LYSE1013>.

644 (58) Guisnet, M. “Ideal” bifunctional catalysis over Pt-acid zeolites. *Catal. Today* **2013**, 218-
645 219, 123–134. DOI: 10.1016/j.cattod.2013.04.028.

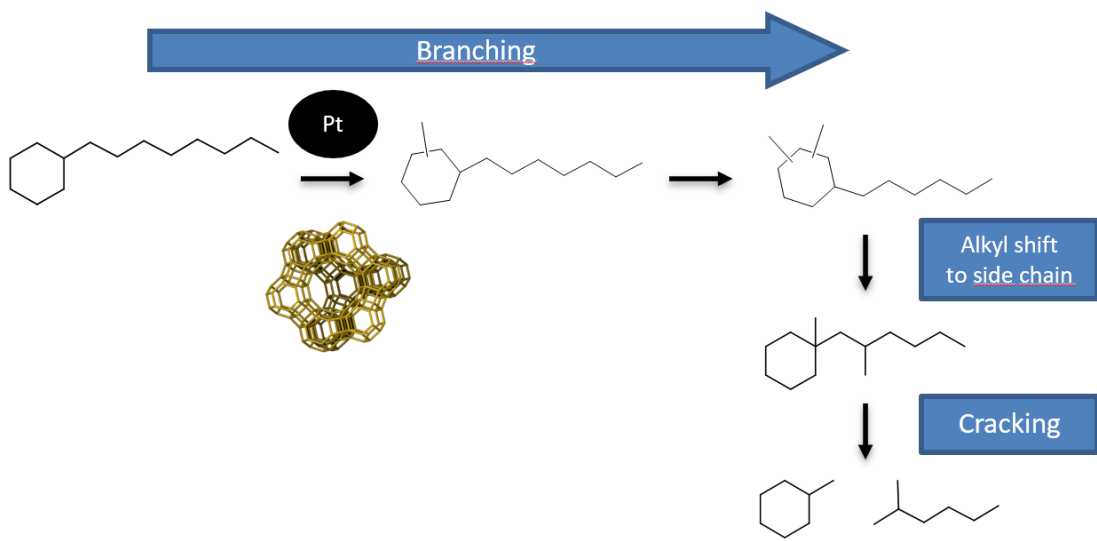
646 (59) McVicker, G. Selective Ring Opening of Naphthenic Molecules. *J. Catal.* **2002**, 210 (1),
647 137–148. DOI: 10.1006/jcat.2002.3685.

648 (60) Martens, G. G.; Marin, G. B.; Martens, J. A.; Jacobs, P. A.; Baroni, G. V. A fundamental
649 kinetic model for hydrocracking of C-8 to C-12 alkanes on Pt/US-Y zeolites. *J. Catal.* **2000**,
650 195 (2), 253–267. DOI: 10.1006/jcat.2000.2993.

651

652

653 TOC Graphic



654

655